

Supporting information for

Coke distribution determines the lifespan of hollow Mo/HZSM-5
capsule catalyst in CH₄ dehydroaromatization

Xin Huang,^{†a} Xi Jiao,^{†c} Mingguo Lin,^{*a} Kai Wang,^{*b} Litao Jia,^a Bo Hou,^a Debao Li^a

^a State Key Laboratory of Coal Conversion, Institute of Coal Chemistry, Chinese Academy of Sciences, Taiyuan 030001, Shanxi, PR China.

^b College of Chemical and Environmental Engineering, Anyang Institute of Technology, Anyang 455000, Henan, PR China.

^c College of Chemistry and Chemical Engineering, Taiyuan University of Technology, Taiyuan 030024, Shanxi, PR China.

Contents

1. Catalyst characterization	3
2. Supplementary Figures S1-S8	5
3. Supplementary Tables S1-S4	13
4. References	15

1. Catalyst characterization

NH₃-TPD: The sample (50 mg) was first heated at 500 °C for 1 h, then cooled to 50 °C in an Ar flow (30 mL/min). Then the sample was exposed to a 10 vol.%NH₃/Ar stream for 1 h at 50 °C. After the NH₃ saturated adsorption, the sample was flushed with Ar flow (30 mL/min) at 120 °C for 1 h, and then heated from 120 °C to 800 °C at a rate of 10 °C/min. A mass spectrometry was used to monitor the NH₃ signal in the reactor effluent.

Py-IR: Approximately 15 mg of sample was first pressed into thin wafers with the diameter of 13 mm. Before the measurement, the sample was evacuated to 10⁻² Pa at 450 °C for 1 h, and IR spectra was then collected at room temperature. Pyridine was introduced into the sample cell until saturation was reached at room temperature. Finally, spectra were then collected after evacuation at 150, 250, and 350 °C, respectively. The concentrations of Lewis and Brønsted acid sites were calculated according to Madeira's paper ^[1].

TPO: The sample at 50 mg was heated in a 10 vol.% O₂/Ar flow of 30 mL/min from room temperature to 750 °C with a rate of 7 °C/min. The mass spectra of gases generated during the TPO were monitored at m/e = 44 (CO₂) and 28 (CO) by a GAM 200 mass spectrometer. The abundance of CO was corrected by subtracting the contribution from the CO₂ abundance, and the abundances of CO and CO₂ were corrected by their respective response parameters ^[2].

TG: Approximately 10 mg of sample was heated from room temperature to 750 °C at a heating rate of 10 °C/min in air flow (30 mL/min).

CH₄ TPSR: The sample (150 mg) was first heated under an Ar flow (30 mL/min) to 500 °C and kept at this temperature for 1 h. After being cooling to room temperature, TPSR was conducted in a pure CH₄ stream (7.5 mL/min) from room temperature to 800 °C at a heating rate of 7 °C/min. During the temperature ramp, MS intensities for 2 (H₂), 16 (CH₄), 27 (C₂H₄), 28 (CO), 30 (C₂H₆), 44 (CO₂), and 78 (C₆H₆) were recorded as a function of temperature ^[3].

In-situ UV-Raman: The coked catalyst (15 mg) was pressed to a dense pellet.

During the in situ UV-Raman analysis, the sample was held by a silver foil, which was secured on the hot stage within the environment chamber ^[4]. The stepwise burn-off of the coking was conducted in a 10 vol.% O₂/Ar flow of 10 mL/min from room temperature to 700 °C with a rate of 7 °C/min. The Raman spectra were collected at room temperature, 400, 450, 500, 550, 600, 650, and 700 °C, respectively.

2. Supplementary Figures S1-S8

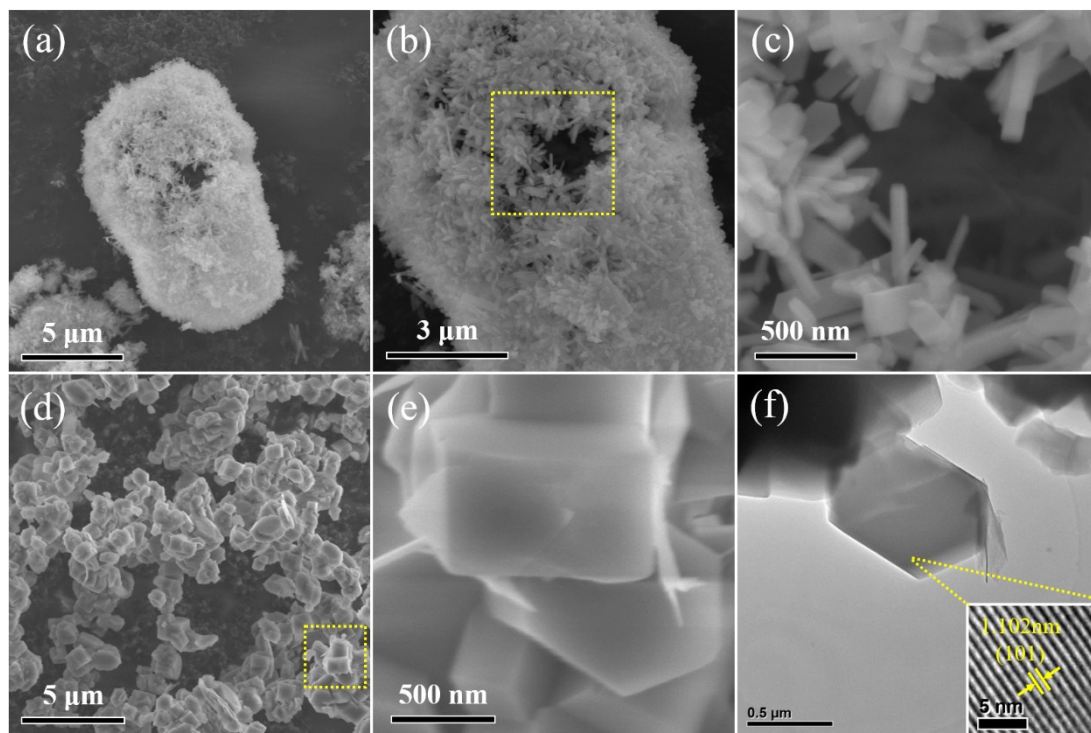


Figure S1 SEM images of the (a, b, c) HC, (d, e) CZ, and (f) TEM image of the CZ support

The commercial HZSM-5 (Si/Al = 30) supplied by Nankai University is frequently chosen as a model support in the MDA reaction in the previous papers [5-7]. So we used this commercial HZSM-5 zeolite as a reference support.

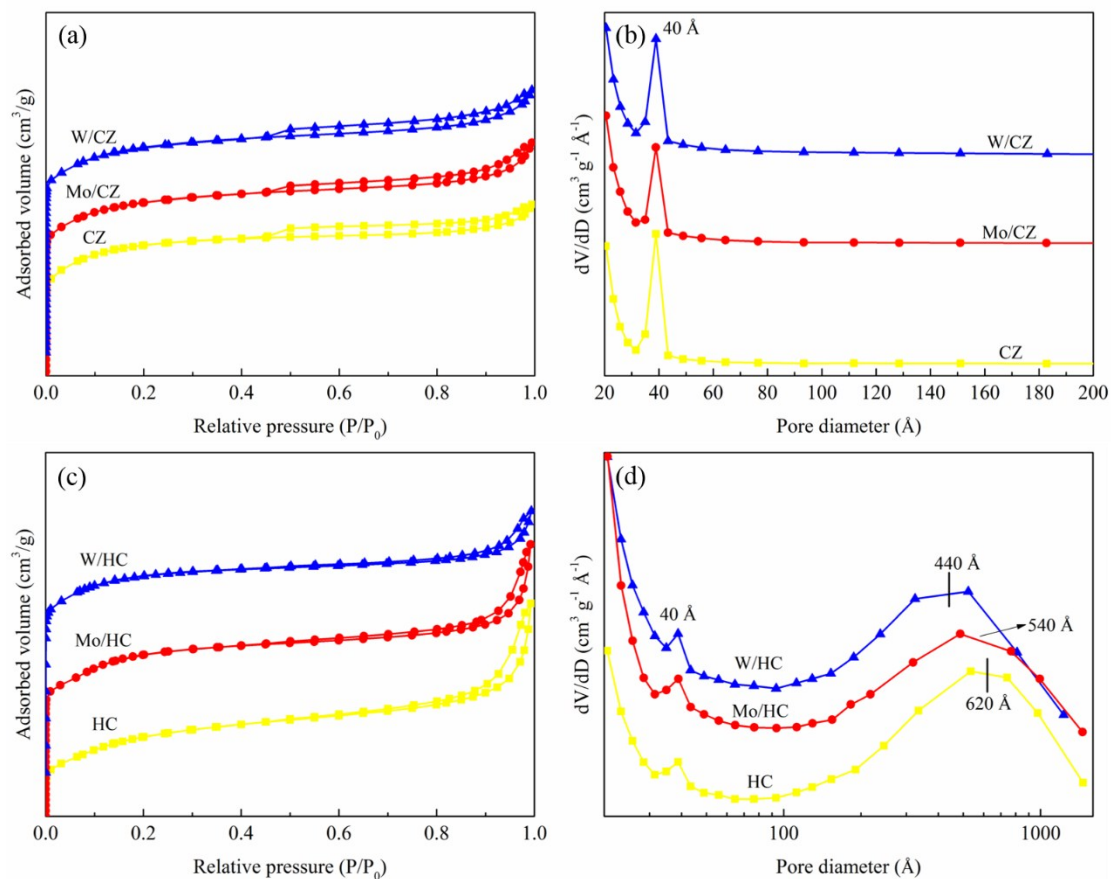


Figure S2 N₂ adsorption-desorption isotherms of the (a) CZ-derived samples and (c) HC-derived samples, pore size distributions of the (b) CZ-derived samples and (d) HC-derived samples

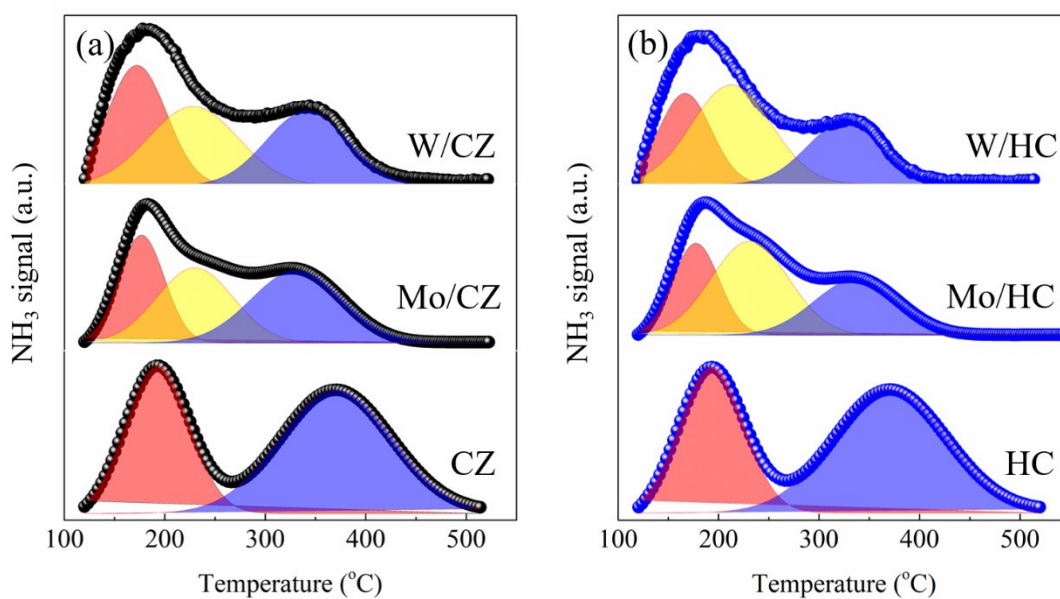


Figure S3 NH₃-TPD profiles of the supports and fresh catalysts

Figure S3 shows both the CZ and HC zeolites possessed double-peak characteristics of zeolites with MFI-structure, and two desorption peaks centered at ca. 190 and 360 °C were assigned to peaks corresponding to weak and strong acid sites, respectively [8]. After Mo/W loading, the peaks areas of the strong acid sites decreased, and a new peak assigned to the medium acid sites (ca. 230 °C) appeared. This revealed that the Mo/W species strongly interacted with strong acid sites and migrate within the zeolite channels to generate medium acid sites [9].

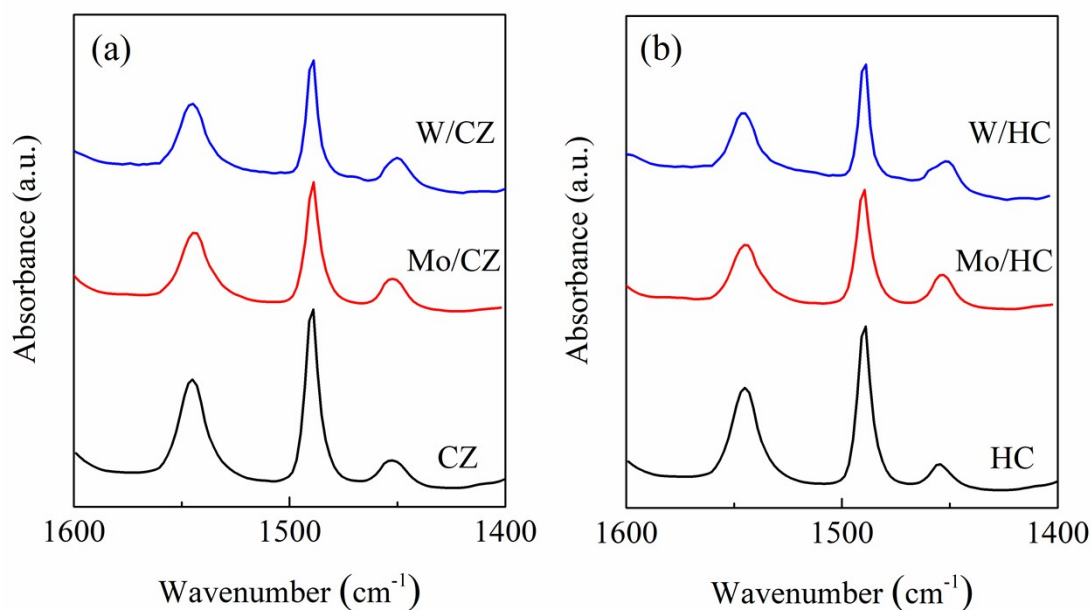


Figure S4 Py-IR spectras of the supports and fresh catalysts

Lewis and Brønsted acid sites can be qualitatively and quantitatively described by Py-IR technique. Figure S4 depicts the bands at ca. 1540 and 1450 cm⁻¹, which were ascribed to Brønsted and Lewis acid sites, respectively, can be observed for all the samples.

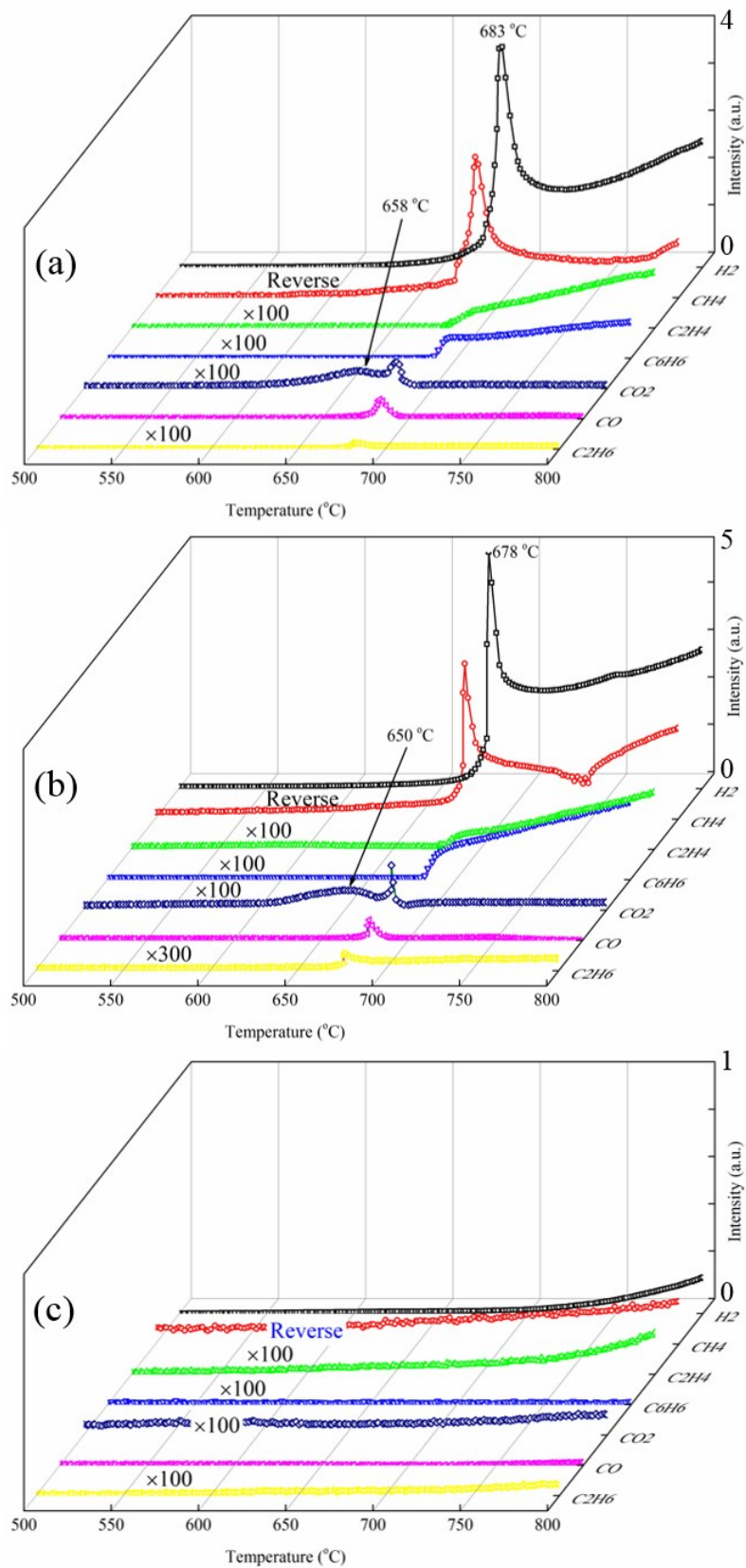


Figure S5 CH₄ TPSR profiles of the fresh (a) Mo/CZ, (b) Mo/HC, and (c) W/CZ catalysts

The formation of various products during the CH₄ TPSR over the Mo/CZ, Mo/HC, and W/CZ catalysts were illustrated in Figure S5. As for the Mo/CZ catalyst, no apparent conversion of methane or formation of any products can be seen below 600 °C. A double-peak feature of CO₂ signal (located at 658 and 683 °C) can be evidently seen, and this stage could be taken as the induction period of the MDA reaction [3]. This suggested that the induction period observed is due to the carbonization of the MoO₃ by methane. Figure S5b shows the carbonizing temperature (650 and 678 °C) of the Mo/HC catalyst was slightly lower than those of the Mo/CZ catalyst, and the signal intensity for both the methane consumption and benzene formation were stronger when compared with the Mo/CZ catalyst. This results revealed that the MDA performance of the hollow Mo/HZSM-5 catalyst is more excellent than that of the commercial Mo/HZSM-5 catalyst.

As for the W/CZ catalyst, no obviously methane consumption or any products can be seen below 700 °C, and the typical double-peak feature of CO₂ formation did not appear below 800 °C. This result verified that W-species over the W/CZ catalyst is hard to be carbonized by methane during the MDA reaction, compared with the two investigated Mo-based catalysts.

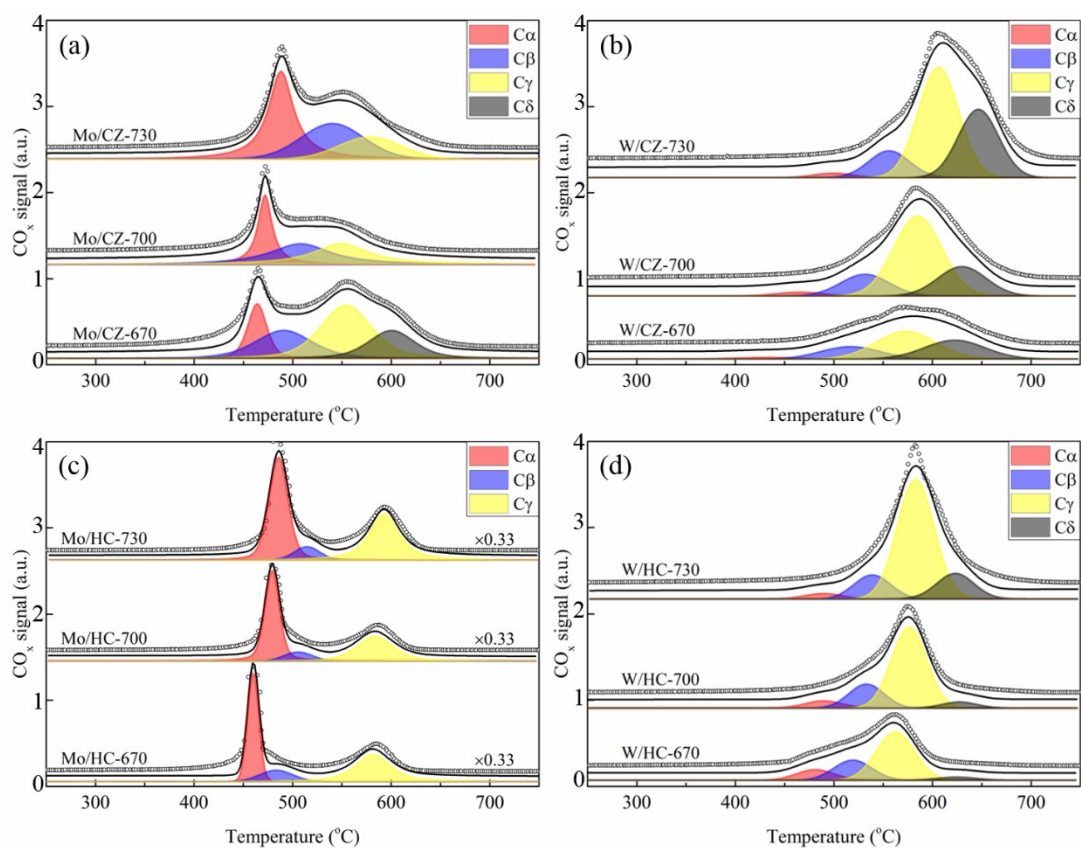


Figure S6 TPO profiles of the used catalysts

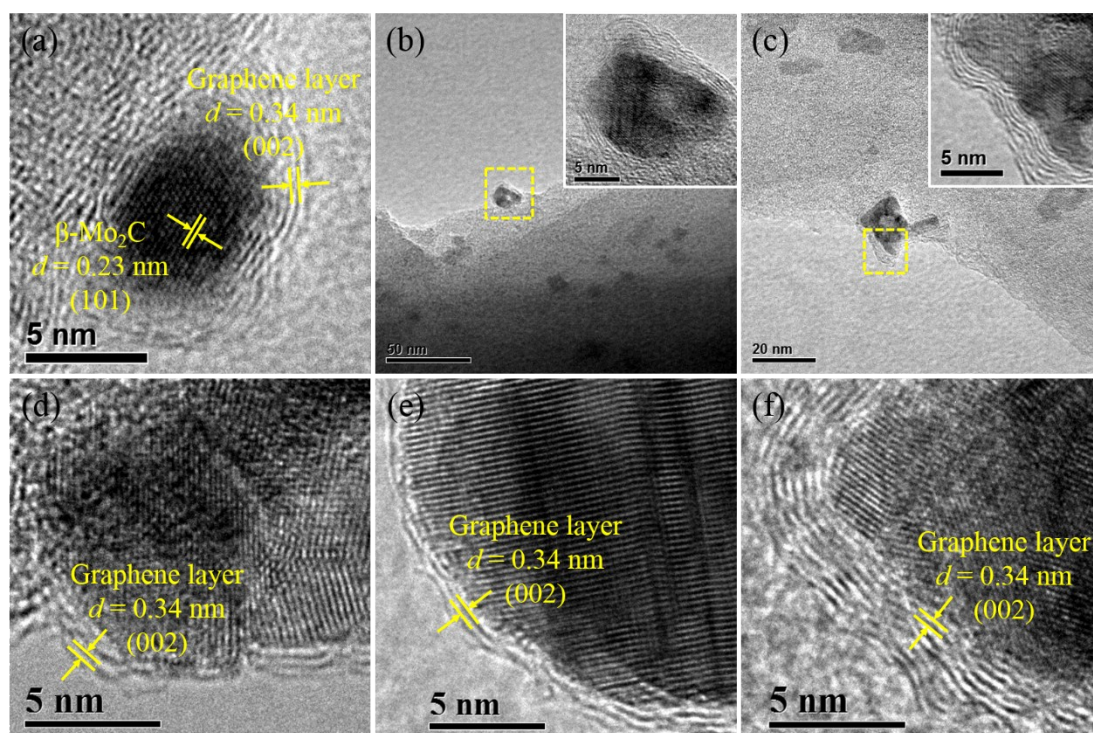


Figure S7 TEM images of the used (a) Mo/CZ-670, (b) Mo/HC-670, (c) Mo/HC-730, (d) W/CZ-670, (e) W/HC-670, and (f) W/HC-730

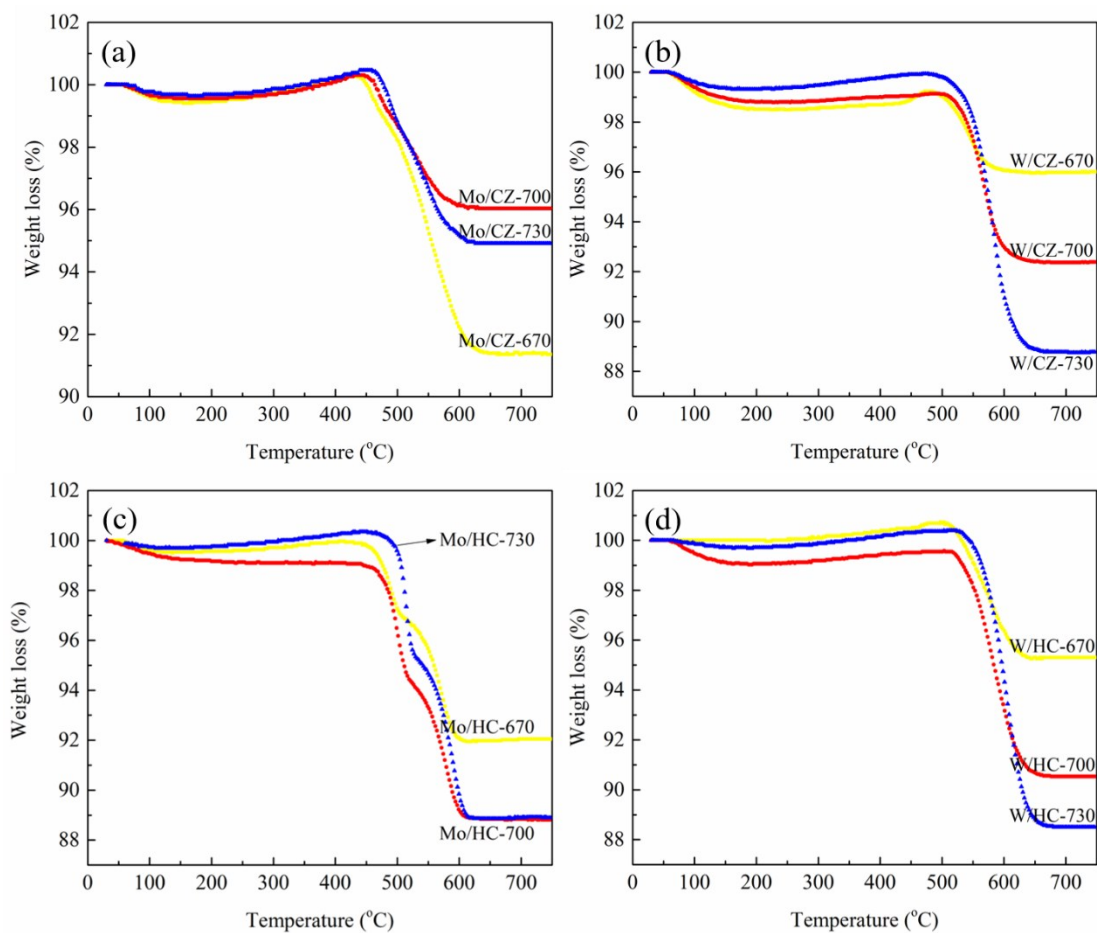


Figure S8 TG profiles of the used catalysts

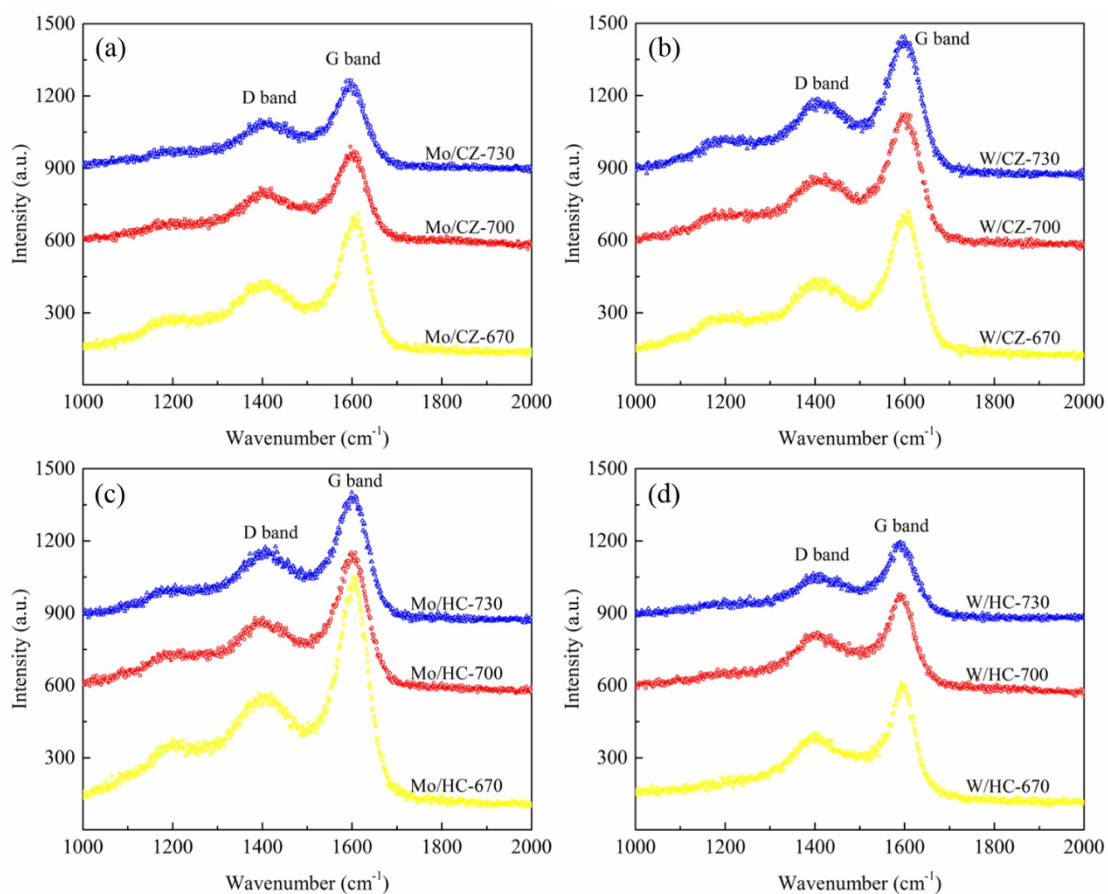


Figure S8 UV-Raman spectra of the used catalysts

As shown in Figure S8, D band (ca. 1350 cm^{-1}) and G band (ca. 1600 cm^{-1}), which can be ascribed to the local disorders of the graphitic structure and C-C vibration of the carbon species with an sp^2 orbital structure, respectively, were visible for all used MDA catalysts ^[10].

3. Supplementary Tables S1-S4

Table S1 ICP-AES analysis for the supports and fresh catalysts

Sample	CZ	Mo/CZ	W/CZ	HC	Mo/HC	W/HC
Si/Al molar ratio	32.2	31.4	31.8	35.4	34.5	33.8
Mo/W content (wt.%)	--	5.9	6.0	--	6.0	6.1

Table S2 Textural properties of the supports, fresh catalysts and used catalysts

Sample	S _{BET} (m ² /g)	S _{micro} (m ² /g)	S _{external} (m ² /g)	V _{micro} (cm ³ /g)	V _{meso} (cm ³ /g)
CZ	384	315	69	0.127	0.059
Mo/CZ	336	260	76	0.106	0.074
Mo/CZ-700	169	124	45	0.048	0.058
W/CZ	345	268	77	0.109	0.073
W/CZ-700	143	113	30	0.044	0.045
HC	350	222	128	0.104	0.141
Mo/HC	266	188	78	0.077	0.140
Mo/HC-700	178	151	27	0.060	0.061
W/HC	270	190	80	0.080	0.139
W/HC-700	233	203	30	0.070	0.099

Table S3 Acidic properties of the supports and fresh catalysts

Sample		CZ	Mo/CZ	W/CZ	HC	Mo/HC	W/HC
NH ₃ -TPD (area)	Strong	33.5	18.3	15.6	31.6	15.7	14.9
	Medium	--	15.9	16.9	--	24.2	25.7
	Weak	22.7	13.7	14.5	21.5	14.2	14.4
Py-IR ($\mu\text{mol/g}$)	Brønsted	312	230	235	305	180	160
	Lewis	56	60	59	54	60	57
	L/B ratio	5.6	3.8	4.0	5.6	3.0	2.8

Table S4 Deactivation rate and average coke formation rate over all the catalysts

Catalysts	Reaction time (h)	Deact. Rate ^c (%/h)	Average coke formation rate (mg/g _{cat} /h)			C _{ex} /C _{in} ratio
			C _{total} ^a	C _{ex} ^b	C _{in} ^b	
Mo/CZ-670	30	0.23	3.01	1.23	1.78	0.69
Mo/CZ-700	14	0.62	3.17	1.96	1.21	1.62
Mo/CZ-730	14	0.70	4.18	3.35	0.83	4.04
Mo/HC-670	50	0.14	1.73	0.97	0.76	1.28
Mo/HC-700	44	0.27	2.61	1.62	0.99	1.63
Mo/HC-730	28	0.46	4.61	2.67	1.94	1.38
W/CZ-670	16	0.20	5.63	2.12	3.51	0.60
W/CZ-700	14	0.43	9.15	2.41	6.74	0.36
W/CZ-730	14	0.70	11.42	1.94	9.48	0.21
W/HC-670	16	0.35	5.13	1.20	3.93	0.31
W/HC-700	14	0.53	9.05	1.72	7.33	0.23
W/HC-730	14	1.09	11.19	1.66	9.53	0.17

^a C_{total} was measured by the TG.

^b Absolute amounts of C α , C β , C γ , and C δ were estimated respectively by multiplying the shares of TPO peak areas to the total coking content by the TG measurement. C_{ex} = C α + C β , and C_{in} = C γ + C δ .

^c Deactivation rate = (CH₄ conversion_{t1} – CH₄ conversion_{t2})/(t2-t1), t1 and t2 represent the time of maximum aromatic yield and finish time, respectively.

4. References

- [1] F. Madeira, K. Tayeb, L. Pinard, H. Vezin, S. Maury, N. Cadran, Ethanol transformation into hydrocarbons on ZSM-5 zeolites: influence of Si/Al ratio on catalytic performances and deactivation rate. Study of the radical species role, *Appl. Catal. A, Gen.* 443-444 (2012) 171-180.
- [2] D. Ma, D. Wang, L. Su, Y. Shu, Y. Xu, X. Bao, Carbonaceous deposition on Mo/HMCM-22 catalysts for methane aromatization: A TP technique investigation, *J. Catal.* 208 (2002) 260-269.
- [3] D. Ma, Y. Shu, M. Cheng, Y. Xu, X. Bao, On the induction period of methane aromatization over Mo-based catalysts, *J. Catal.* 194 (2000) 105-114.
- [4] X. Li, M. Liu, S. Lai, D. Ding, M. Gong, J. Lee, K. Blinn, Y. Bu, Z. Wang, L. Bottomley, F. Alamgir, M. Liu, In situ probing of the mechanisms of coking resistance on catalyst-modified anodes for solid oxide fuel cells, *Chem. Mater.* 27 (2015) 822-828.
- [5] D. Ma, Y. Shu, X. Bao, Y. Xu, Methane dehydro-aromatization under nonoxidative conditions over Mo/HZSM-5 catalysts: EPR study of the Mo species on/in the HZSM-5 zeolite, *J. Catal.* 189 (2000) 314-325.
- [6] H. Zheng, D. Ma, X. Liu, W. Zhang, X. Han, Y. Xu, X. Bao, Methane dehydroaromatization over Mo/HZSM-5: A study of catalytic process, *Catal. Lett.* 111 (2006) 111-114.
- [7] P. Tan, The catalytic performance of Mo-impregnated HZSM-5 zeolite in CH₄ aromatization: Strong influence of Mo loading and pretreatment conditions, *Catal. Commun.* 103 (2018) 101-104.
- [8] R. Long, R. Yang, Temperature-programmed desorption/surface reaction (TPD/TPSR) study of Fe-exchanged ZSM-5 for selective catalytic reduction of nitric oxide by ammonia, *J. Catal.* 198 (2001) 20-28.
- [9] Y. Liu, M. Zhao, L. Cheng, J. Yang, L. Liu, J. Wang, D. Yin, J. Lu, Y. Zhang, Facile synthesis and its high catalytic performance of hierarchical ZSM-5 zeolite from economical bulk silicon oxides, *Micro. Meso. Mater.* 260 (2018) 116-124.

[10]X. Huang, C. Ji, C. Wang, F. Xiao, N. Zhao, N. Sun, W. Wei, Y. Sun, Ordered mesoporous CoO-NiO-Al₂O₃ bimetallic catalysts with dual confinement effects for CO₂ reforming of CH₄, Catal. Today 281 (2017) 241-249.